$Y_2Si_3O_3N_4:Ce^{3+}$: a promising phosphor for WLEDs in general lighting applications

H. M. TRUNG[1], N. T. D. AN[2], N. L. THAI[3,*], H. Y. LEE[4]
[1]*Faculty of Basic Sciences, Vinh Long University of Technology Education, Vinh Long Province, Vietnam*
[2]*Faculty of Electrical Engineering Technology, Industrial University of Ho Chi Minh City, Ho Chi Minh City, Vietnam*
[3]*Faculty of Engineering and Technology, Nguyen Tat Thanh University, Ho Chi Minh City, Vietnam*
[4]*Department of Electrical Engineering, National Kaohsiung University of Sciences and Technology, Kaohsiung, Taiwan*

The blue-green emitting phosphor $Y_2Si_3O_3N_4:Ce^{3+}$, with strong absorption well matching with the near-UV excitation of the LED, is produced using solid-state synthesis. The characterization analysis of the prepared phosphor shows that $Y_2Si_3O_3N_4:Ce^{3+}$ with 0.06 doping concentration of Ce^{3+} ion presents significant absorption centered at 397 nm and broad emission range from blue to green under the near-UV excitation. The large emission wavelength band (456 nm – 500 nm) of Ce^{3+}-doped $Y_2Si_3O_3N_4$ could be owing to the transition from 5d to 4f energy levels of Ce^{3+} ions. The phosphor is incorporated as the second phosphor material, with yellow-emitting phosphor YAG:Ce^{3+}, to fabricate a single white light-emitting diode (W-LED) structure. The impacts of doping $Y_2Si_3O_3N_4:Ce^{3+}$ on the lighting efficiency of the W-LED are investigated. The luminous intensity and color temperature consistency are generally benefitted from the increase of $Y_2Si_3O_3N_4:Ce^{3+}$ doping concentration. Conversely, the color rendering indices tend to favor the lower concentration of $Y_2Si_3O_3N_4:Ce^{3+}$. The blue-green emitting phosphor $Y_2Si_3O_3N_4:Ce^{3+}$, therefore, can be promising for high-flux lighting applications that require relatively good chromatic rendition.

(Received May 16, 2022; accepted October 9, 2023)

Keywords: White LED, Lambert-Beer law, Color rendering index, Luminous efficacy

1. Introduction

Energy-consumption reduction and environmental protection have been focused on in many industries, and the lighting industry is not exceptional [1, 2]. The white light emitting diode, W-LED, has emersed as a promising lighting solution to alternate the traditional illuminating tubes. This kind of light source is also well-known for its high lumen efficiency, low power consumption, remarkable robustness and resistance, and long lifetime that is estimated around 50,000 hours [3, 4]. Moreover, the W-LED does not use mercury in production thus it can significantly reduce the pollutant emitted to the environment. This means the W-LED is an outstanding source for the lighting market and industry to address the two mentioned issues [5]. Therefore, heightened expectations for LED production have been realized, leading to extensive researches on approaches to achieve appropriate material and building construction of W-LEDs. The W-LED is usually fabricated by combining three LED chips with different emission colors of green, blue and red to generate white light [6-8]. Besides, to reduce the complexity in structuring, the combination of LED chips and one or more phosphor materials is proposed as an alternative to the former [9]. With the simple fabrication and easier approach to enhance the performance of the total W-LED package, which is exploring the suitable phosphor types, it is popular to apply the LED chip – phosphor combination to large-scale production.

The very first applied phosphor is the yellow-emitting phosphor YAG:Ce^{3+}, which has been recognized for the high luminescence efficiency. The well-known drawback of this phosphor is the low color rendering efficiency. Other oxide- and sulfur-based phosphors have been proposed for red spectral compensation, yet their luminescence is degraded in high moisture and high temperature environments. Developing a phosphor exhibiting high stability in chemical features, strong luminescent output, and harmless to environments is desirable [10-12]. Additionally, the prepared phosphor needs to present a broad emission wavelength that overlaps the excitation spectrum in near-UV/blue wavelength bands for high absorption and conversion efficiency. Consequently, the large crystal field of phosphor hosts has drawn significant attention. (Oxy)nitride phosphors are noticed because of their stability in chemical and thermal factors [13, 14]. Besides, its red shift in emission is large enough to cover the spectrum wavelength of 500 nm. Besides, the dopant of rare-earth ions of Ce^{3+} is reported to possess broad-band emission wavelength obtained from the transition of 5d excited state to 4f ground state, small Stoke shift, and short decay time [15]. Besides, the centers of emission and excitation bands of the doped ions are dependent on crystal geometries and the site environments of the host, thus emission can be tunable from blue to red in the (oxy)nitride-silicon host [16-18]. Accordingly, the Ce^{3+} ion might be suitable rare-earth dopants for (oxy)nitride hosts.

$Y_2Si_3O_3N_4:Ce^{3+}$ was reported as a promising phosphor, which exhibited bright blue emission and strong absorption within near-UV regions, for W-LEDs in general lighting applications [19, 20]. In this work, this blue-emitting phosphor synthesis is carried out via the solid state reaction method. The photoluminescence properties of the phosphor that depend on the concentration of Ce^{3+} dopants are analyzed and presented in the next section. Subsequently, the investigation of the lighting properties, dependent on the doping concentration of $Y_2Si_3O_3N_4:Ce^{3+}$ in the phosphor packages of the W-LED, is demonstrated [21, 22]. The results show that $Y_2Si_3O_3N_4:Ce^{3+}$ presents broad and intense emission covering the blue-green wavelength region, indicating that it is appropriate to be applied in high-luminescence WLEDs for general illumination or display devices.

2. Phosphor characterization

When being excited in a near-UV region, the strong emission of $Y_2Si_3O_3N_4:Ce^{3+}$ can be obtained. Moreover, the emission band of the phosphor overlaps the emission range of 465 – 500 nm due to the transition of the Ce^{3+} from 5d excited state to 4f ground state. The emission peak of $Y_2Si_3O_3N_4:Ce^{3+}$ changes with the doping concentration of Ce^{3+}. As the concentration of the dopant increases, the increase in the phosphor emission strength can be observed. The highest emission strength is obtained when the concentration of Ce^{3+} is about 0.06. Then, it starts to fall when Ce^{3+} concentration is > 0.06, attributed to the concentration quenching influence. The emission peak at 456 nm is observed with 0.02 Ce^{3+} and gradually broadens to 500 nm when doping Ce^{3+} at 0.4. The red-shift of the photoluminescence of $Y_2Si_3O_3N_4:Ce^{3+}$ could be demonstrated by the energy transfer between Ce^{3+} ions, owing to the decrease in the energy levels of the 5d orbitals caused by the high probability of changing the strength of crystal field surround the ion Ce^{3+}.

The absorption of the 0.06 Ce^{3+}-doped $Y_2Si_3O_3N_4$ is monitored with the excitation and emission wavelengths of 397 nm and 505 nm, respectively. The phosphor shows intense absorption region that peak at 397 nm, indicating great overlap with a near-UV excitation band. This may be ascribed to the 4f → 5d transitions of the Ce^{3+} allowed by the electronic dipole interactions. Besides, the transitions from the lowest excited state of 5d orbitals to the ground state of $^2F_{5/2}$ and $^2F_{7/2}$ can get the asymmetric emission spectrum divided into two Gaussian peaks at 465 nm and 505 nm, respectively. Moreover, the well-matching status between the lowest excitation and greatest emission ranges implies the significant energy transfer probability of an ion Ce^{3+} to another one in the host lattice. With the increasing concentration of Ce^{3+} dopants, the distance among Ce^{3+} ions becomes narrower, and thus the energy transfer among them could be better.

The energy transfer of Ce^{3+} ions is validated by the photoluminescence decay curves of the Ce^{3+}-doped $Y_2Si_3O_3N_4$ phosphor. The curves are computed with the excitation wavelength of 397 nm and the emission wavelength of 465 nm and fitted with a second-order exponential decay function [23, 24].

$$I = A_1 \exp\left(\frac{-t}{\tau_1}\right) + A_2 \exp\left(\frac{-t}{\tau_2}\right) \quad (1)$$

I indicates the intensity of the luminous output, A_1 and A_2 are constants, t shows the time, and τ_1 and τ_2 indicate the fast and slow decay lifetimes of the exponential factors.

The critical distance of Ce^{3+} energy transfer could be estimated following Blasse's research work [25, 26].

$$R_c = 2\left(\frac{3V}{4\pi x_c Z}\right)^{\frac{1}{3}} \quad (2)$$

R_c is the critical distance among the ions Ce^{3+}, V is the unit cell's volume, and x_c presents the critical concentration. With the concentration of Ce^{3+} x_c = *0.06*, and the values of V and Z are 290.42 $Å^3$ and 2, respectively, the calculated critical distance R_c is 17 Å.

The energy transfer between Ce^{3+} ions is also allowed by the dipole-dipole interaction, based on the nonradiative energy transfer of Dexter's work, the critical distance R_c could be expressed as the following equation [27, 28].

$$R_c = 0.63\times10^{28}\times4.8\times10^{-16}\times f\times\frac{SO}{E^4} \quad (3)$$

f shows the oscillator strength for the transition of the Ce^{3+} ions, E indicates the energy of the highest spectral overlap, and SO is the overlap of the high energy emission spectrum and the low energy excitation spectrum of the Ce^{3+} ions. Here, f determined to be 10^{-2} for the broad absorption range of 4f → 5d, E = 2.85 eV, and SO = 0.71 eV^{-1}. Consequently, R_c = 19 Å can be obtained [29].

Considering the obtained results, the computation carried out with the structural and critical concentration parameters shows the result that well overlaps with experimental spectra statistics, meaning that the Ce^{3+} energy transfer in the $Y_2Si_3O_3N_4$ host mainly takes place via the electrostatic interaction.

3. Analysis and discussion

The concentration of $Y_2Si_3O_3N_4:Ce^{3+}$ has certain effects on the power output of WLED phosphor configuration. With 5 wt% and 10 wt% of the blue phosphors applied, the sum power of WLED packages performs differently, as displayed in Fig. 1. At each preset correlated color temperature CCT value, the concentration-depending intensity of sum power is different. At a low CCT of 3000 K, the power intensity of the lower concentration is much stronger while at the other higher CCTs, the difference is insignificant. The noticeable point is that at both higher CCT values, 5 wt%

still performs better results, in terms of boosting the spectral energy of the blue region (450-465 nm). Particularly, at 4000 K, the intensity in the blue region shows a little enhancement. In the case of 5000 K, the blue intensity is remarkable with two doping concentrations of $Y_2Si_3O_3N_4:Ce^{3+}$ but the line of 5 wt% is somehow better. Meanwhile, for the green region (495-570 nm), the 10 wt% can be more favorable. This implies that the phosphor can be suitable for utilization in WLED to achieve a good cover of the emission spectra of both blue and green ranges (450 nm and 500 nm). These two spectral regions contribute greatly to the performance of luminescence and chromaticity characteristics of the WLED. The power increases attained in these regions could promote the lumen output of the WLED packages, and so does the blue-light scattering efficiency. Generally, the WLED with the high requirement in color rendering factors will exhibit a minor decrease in the luminous intensity. If the scattering is too strong, it will be a defect to the luminous output but an advantage to the color rendition.

The scattering influences regarding the concentration of blue-green emitting phosphor $Y_2Si_3O_3N_4:Ce^{3+}$ can be implied from the changes in yellow-emitting $YAG:Ce^{3+}$ phosphor concentration. Fig. 2 shows the changes in yellow phosphor concentration with 5 wt% and 10 wt% of $Y_2Si_3O_3N_4:Ce^{3+}$ at 3000 K, 4000 K and 5000 K. The higher concentration (10 wt%) obviously causes the decreasing concentration of the yellow phosphor. This means the increase of $Y_2Si_3O_3N_4:Ce^{3+}$ concentration could lead to the decrease of $YAG:Ce^{3+}$ concentration. The two points might be implied from this change are the preserved CCT stability and the boosted scattered light events. This could reduce the back-scattering effect and the energy loss caused by internal reflection [30, 31]. Also, the conversion efficiency of blue-light emission is stimulated, and the light is redirected in a straight path for better extraction performance. This eventually enhances the light emission and affects the chromaticity factors.

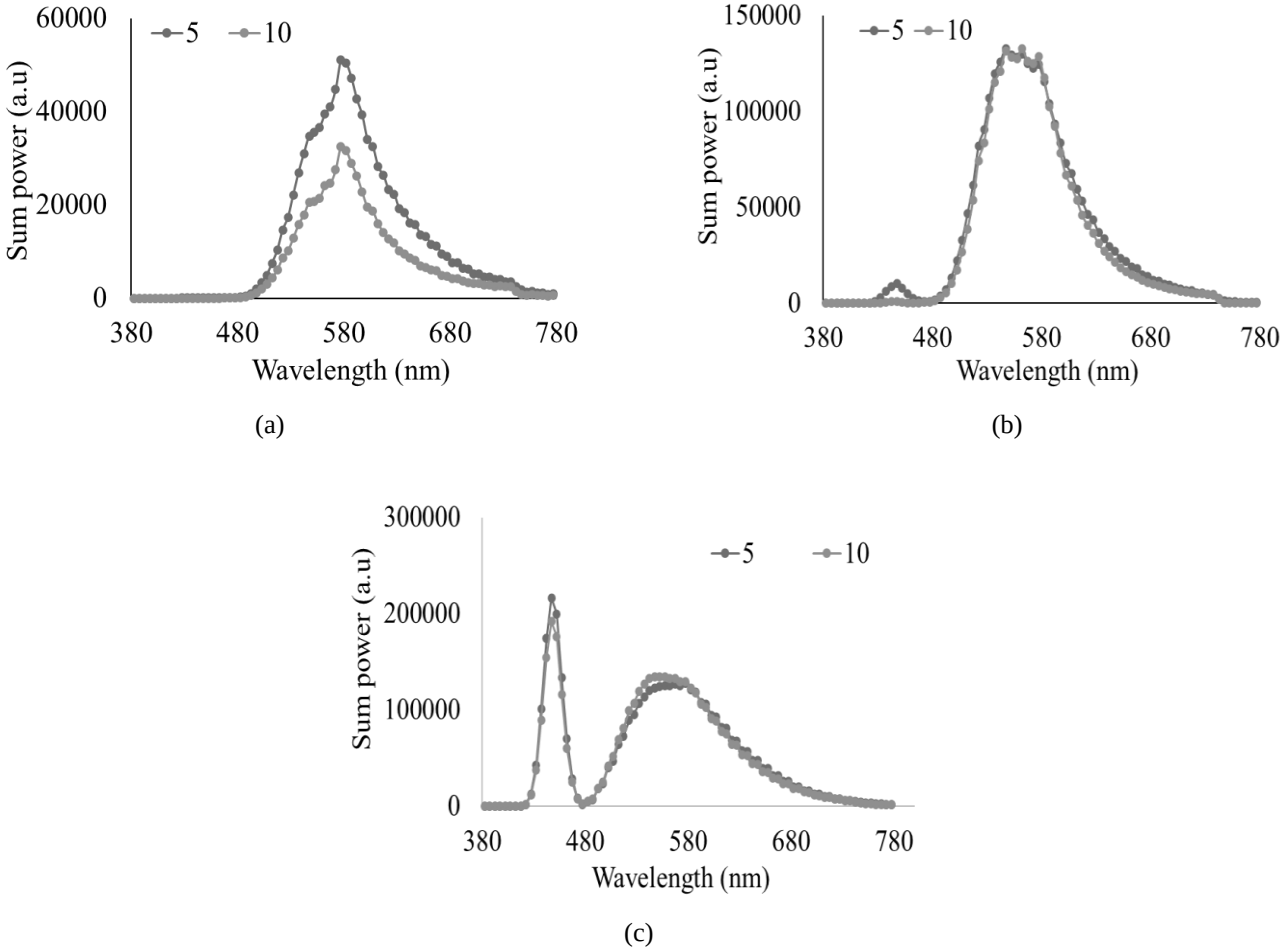

Fig. 1. Sum power of WLEDs as a function of blue phosphor concentrations: (a) 3000 K; (b) 4000 K; (c) 5000 K

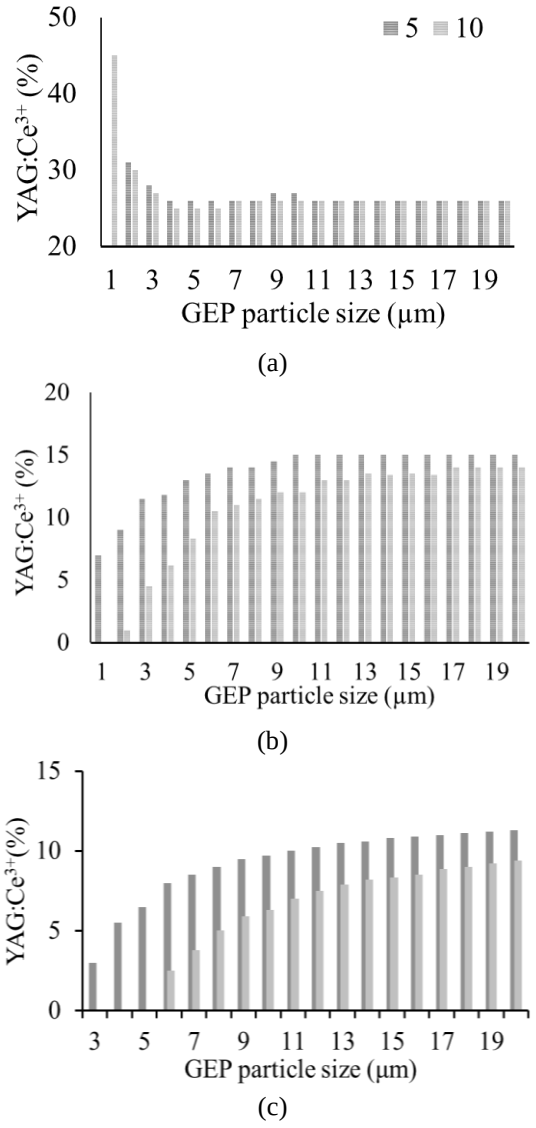

Fig. 2. YAG:Ce^{3+} changing concentrations as a function of blue phosphor concentrations: (a) 3000 K; (b) 4000 K; (c) 5000 K

The scattering enhancement benefits both luminous flux and color uniformity. Apart from the concentration, the particle size also impacts the luminous efficiency, which can be seen in Fig. 3. At 3000 K (Fig. 3a) the higher concentration is not favorable but the larger particle size is. Meanwhile, at 4000 K and 5000 K CCTs of WLEDs (Fig. 3c–d), $Y_2Si_3O_3N_4:Ce^{3+}$ higher concentration is likely to heighten the luminous flux while the effect of the particle size is not too significant. Combining the results in Fig. 3 with those in Fig. 2, this could be attributed to the fluctuation of the yellow-emitting phosphor concentration. The concentration of YAG:Ce^{3+} in the WLED with 5000 K in Fig. 2c, for example, is lower in the case of 10 wt% $Y_2Si_3O_3N_4:Ce^{3+}$, yet the larger particle size of this phosphor causes the concentration of yellow phosphor to increase. Thus, at 5000 K (Fig. 3c), the luminous flux of the WLED is higher with increasing concentration of the blue-green emitting phosphor but slightly decreases with its larger sizes (at the same concentration level).

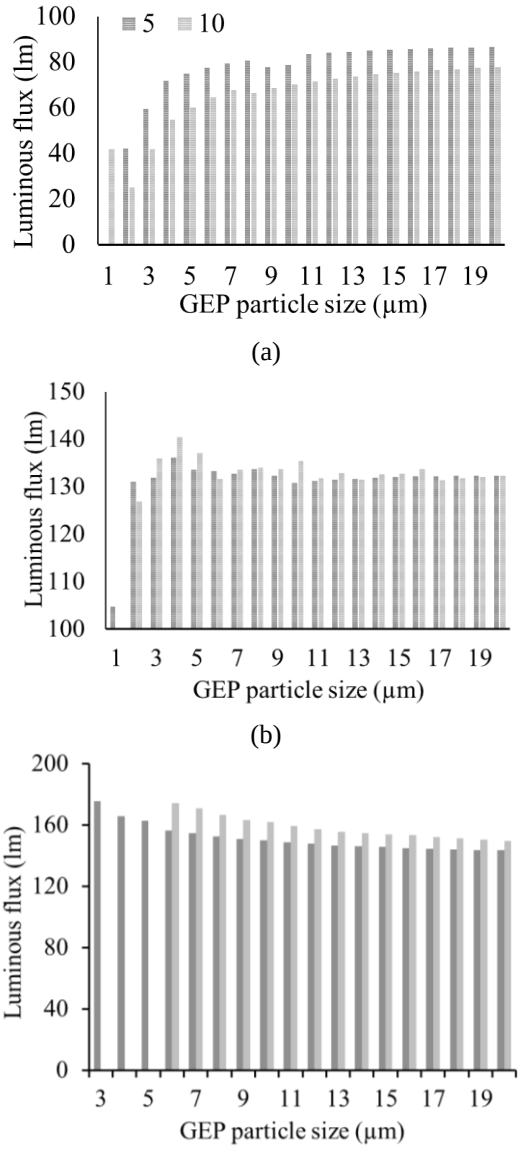

Fig. 3. LF values of WLEDs as a function of blue phosphor concentrations: (a) 3000 K; (b) 4000 K; (c) 5000 K

The function of $Y_2Si_3O_3N_4:Ce^{3+}$ in maintaining the stability of color temperatures for the WLEDs is presented clearly in Fig. 4. As can be seen, the concentration of this blue-green emitting phosphor greatly affects the CCT fluctuation of the WLED. In Fig. 4a, the lower concentration of the phosphor $Y_2Si_3O_3N_4:Ce^{3+}$ (5 wt%) shows smaller differences between the CCT values in certain angles. Particularly, the CCT remained at 3000 K with negligible fluctuation in the viewing angle from -60° to 60°. In Fig. 4c and d, the CCTs with 10 wt% $Y_2Si_3O_3N_4:Ce^{3+}$ are more stable than the ones with 5 wt%,

as a smaller deviation can be observed. This might also be ascribed to the changes in yellow phosphor concentration. Besides, the absorption characteristics of the blue-green phosphor $Y_2Si_3O_3N_4:Ce^{3+}$ contributes to the conversion efficiency of light. The yellow light will be absorbed once it reaches the $Y_2Si_3O_3N_4:Ce^{3+}$ phosphor that finally converts them into blue light and a small proportion of green light. This means the blue and green light emission colors increase, contributing to balance the proportion of each color element of white light including blue, green, and yellow. Consequently, color uniformity can be obtained.

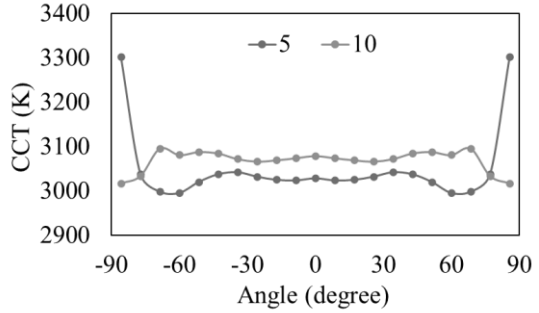

(a)

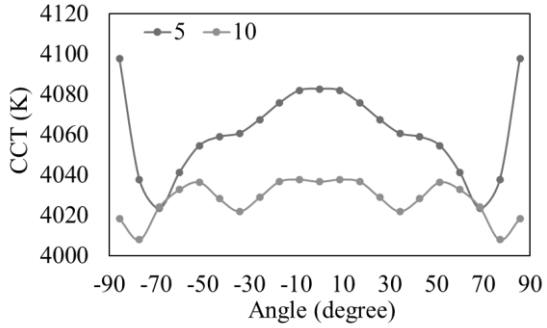

(b)

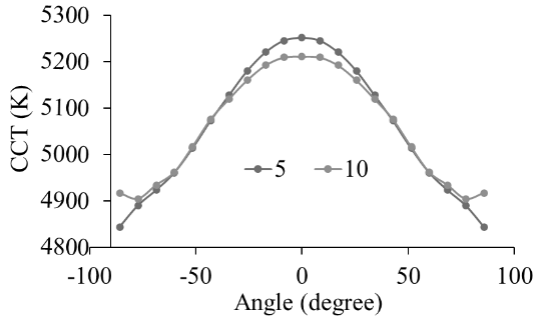

(c)

Fig. 4. CCT values of WLEDs as a function of blue phosphor concentrations: (a) 3000 K; (b) 4000 K; (c) 5000 K

Color uniformity is regarded as one of the essential factors to evaluate the chromatic quality of the white light from LED lamps. It is important to assess the color reproduction of the light source toward a specific subject. At this point, both CRI – short for color rendering index and CQS – short for color quality scale are selected. CRI and CQS values of WLEDs with different concentrations of $Y_2Si_3O_3N_4:Ce^{3+}$ phosphor are presented in Figs. 5 and 6, respectively.

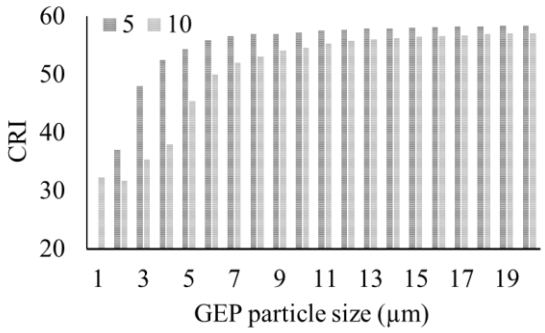

(a)

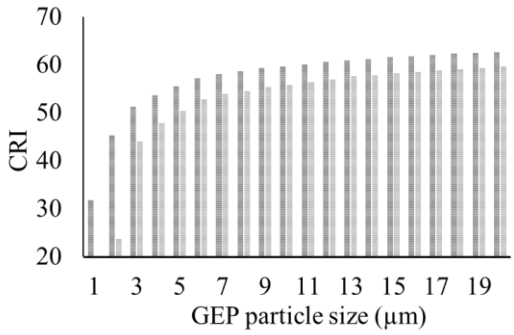

(b)

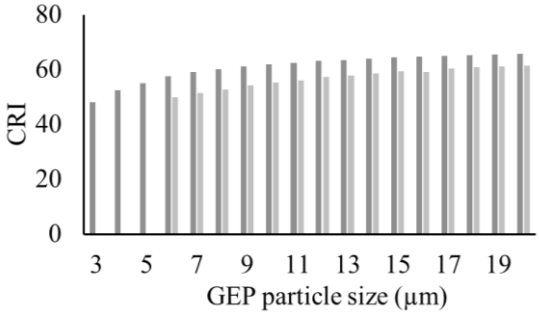

(c)

Fig. 5. CRI values of WLEDs as a function of blue phosphor concentrations: (a) 3000 K; (b) 4000 K; (c) 5000 K

The changes in CRI and CQS with the increasing concentration of the blue-green emitting phosphor are similar. The higher the proportion of $Y_2Si_3O_3N_4:Ce^{3+}$ in the phosphor package, the lower the CRI and CQS become. The highest CRI and CQS at three CCT values are in the range of 60 - 64 with 5 wt% $Y_2Si_3O_3N_4:Ce^{3+}$. Studies pointed out the drawbacks of CRI in the color fidelity of a white light source, which is that even the light source of too high red or blue color spectral energies is possible to perform high CRI [33-35]. Moreover, the small

number of assessing color samples, 8 color samples, limits the accuracy of chromatic reproduction. The CQS, on the other hand, allows the color to be reproduced on a larger range of color samples, 15 color samples, thus the accuracy can be significantly higher. Furthermore, the CQS evaluates not only the CRI, but also the visual preferences of humans and the color coordination factors. Therefore, the WLED with strong luminous intensity and moderate CQS is more desirable, in terms of WLED devices for display applications [32]. This work has presented that the blue-green emitting phosphor $Y_2Si_3O_3N_4:Ce^{3+}$ is potential material for manufacturers to fulfill this desire.

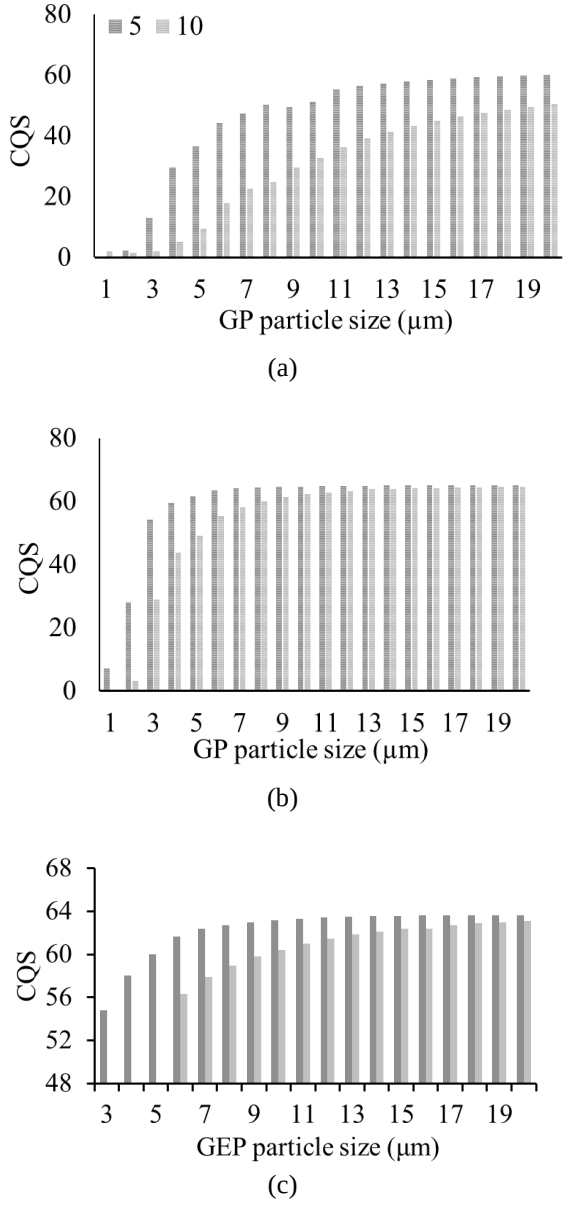

Fig. 6. CQS values of WLEDs as a function of blue phosphor concentrations: (a) 3000 K; (b) 4000 K; (c) 5000 K

4. Conclusions

This paper shows the potential of the blue-green emitting phosphor of $Y_2Si_3O_3N_4:Ce^{3+}$ in performing good color adequacy and strong luminosity for WLED models. $Y_2Si_3O_3N_4:Ce^{3+}$ phosphor exhibits broad and intense emission with a good overlap over the blue-green wavelength region. When being applied to the phosphor packages of the WLED structures, the varying concentrations of the phosphor have significant impacts on the luminous intensity and color fidelity of the WLED. The lower concentration of 5 wt.% benefits the CQS and CRI while the higher concentration of 10 wet% is more favorable to the consistency of the CCT, or color uniformity, and luminous flux. This could be attributed to the decrease of yellow-emitting phosphor YAG:Ce^{3+} concentration to stimulate the forward-scattering probability and reduce the back-scattering as well as the internal reflection to limit the lighting energy loss and low light extraction. Depending on the choice of the manufacturers, it is acceptable to have a minor reduction in color performance or luminous flux to fulfill their goals.

References

[1] L. Qin, X. Shi, A. S. Leon, Appl. Opt. **59**, 683 (2020).
[2] W. Tian, L. Dou, Z. Jin, J. Xiao, J. Li, Appl. Opt. **59**, 11112 (2020).
[3] K. Zhang, H. Lu, L. Shao, C. Zheng, Y. Zhang, S. Huang, J. Opt. Technol. **88**, 548 (2021).
[4] H. Li, P. Li, H. Zhang, Y. C. Chow, M. S. Wong, S. Pinna, J. Klamkin, J. S. Speck, S. Nakamura, S. P. DenBaars, Opt. Express **28**, 13569 (2020).
[5] B. Jain, R. T. Velpula, H. Q. T. Bui, H. D. Nguyen, T. R. Lenka, T. K. Nguyen, H. P. T. Nguyen, Opt. Express **28**, 665 (2020).
[6] K. J. Singh, X. Fan, A. S. Sadhu, C. H. Lin, F. Liou, T. Wu, Y. Lu, Jr. He, Z. Chen, T. Wu, H. Kuo, Photon. Res. **9**, 2341 (2021).
[7] L. Shi, X. Zhao, P. Du, Y. Liu, Q. Lv, S. Zhou, Opt. Express **29**, 42276 (2021).
[8] S. Shadalou, W. J. Cassarly, T. J. Suleski, Opt. Express **29**, 35755 (2021).
[9] S. Hsin, C. Hsu, N. Chen, C. Ye, G. Ji, K. Huang, H. Hsieh, C. Wu, C. Dai, Appl. Opt. **60**, 7775 (2021).
[10] X. Yu, L. Xiang, S. Zhou, N. Pei, X. Luo, Appl. Opt. **60**, 306 (2021).
[11] C. Zhang, B. Yang, J. Chen, D. Wang, Y. Zhang, S. Li, X. Dai, S. Zhang, M. Lu, Opt. Express **28**, 194 (2020).
[12] D. T. Tuyet, V. T. H. Quan, B. Bondzior, P. J. Dereń, R. T. Velpula, H. P. T. Nguyen, L. A. Tuyen, N. Q. Hung, H. D. Nguyen, Opt. Express **28**, 26189 (2020).
[13] H. Yuce, T. Guner, S. Balci, M. M. Demir, Opt. Lett. **44**, 479 (2019).
[14] H. Shih, C. Liu, W. Cheng, W. Cheng, Opt. Express **28**, 28218 (2020).
[15] L. Ma, Y. Zhao, M. Du, X. Pei, X. Feng, F. Sun, S. Fang, Appl. Opt. **60**, 6030 (2021).

[16] Y. Zhang, Z. Yu, X. Xue, F. Wang, S. Li, X. Dai, L. Wu, S. Zhang, S. Wang, M. Lu, Opt. Express **29**, 34126 (2021).
[17] S. Yigen, M. Ekmekcioglu, M. Ozdemir, G. Aygun, L. Ozyuzer, Appl. Opt. **60**, 8949 (2021).
[18] B. Yu, S. Liang, F. Zhang, Z. Li, B. Liu, X. Ding, Photon. Res. **9**, 1559 (2021).
[19] P. Liu, Z. Guan, T. Zhou, Q. Xie, Q. Yu, Y. He, Z. Zeng, X. Wang, Appl. Opt. **60**, 5652 (2021).
[20] S. Kumar, M. Mahadevappa, P. K. Dutta, Appl. Opt. **58**, 509 (2019).
[21] J. Chen, Y. Tang, X. Yi, Y. Tian, G. Ao, D. Hao, Y. Lin, S. Zhou, Opt. Mater. Express **9**, 3333 (2019).
[22] G. Xia, Y. Ma, X. Chen, S. Q. Jin, C. Huang, J. Opt. Soc. Am. **A 36**, 751 (2019).
[23] A. Adnan, Y. Liu, C. Chow, C. Yeh, OSA Continuum **3**, 1163 (2020).
[24] Y. Jen, X. Lee, S. Lin, C. Sun, C. Wu, Y. Yu, T. Yang, OSA Continuum **2**, 2460 (2019).
[25] J. Chen, B. Fritz, G. Liang, X. Ding, U. Lemmer, G. Gomard, Opt. Express **27**, A25 (2019).
[26] T. Ya. Orudzhev, S. G. Abdullaeva, R. B. Dzhabbarov, J. Opt. Technol. **86**, 671 (2019).
[27] H. Jin, L. Chen, J. Li, X. An, Y. P. Wu, L. Zhu, H. Yi, K. H. Li, Opt. Lett. **45**, 6671 (2020).
[28] Z. Li, J. Zheng, J. Li, W. Zhan, Y. Tang, Opt. Express **28**, 13279 (2020).
[29] N. Bamiedakis, J. J. D. McKendry, E. Xie, E. Gu, M. D. Dawson, R. V. Penty, I. H. White, J. Lightwave Technol. **37**, 3305 (2019).
[30] P. Zhu, H. Zhu, S. Thapa, G. C. Adhikari, Opt. Express **27**, A1297 (2019).
[31] N. A. Mica, R. Bian, P. Manousiadis, L. K. Jagadamma, I. Tavakkolnia, H. Haas, G. A. Turnbull, I. D. W. Samuel, Photon. Res. **8**, A16 (2020).
[32] C. Lin, A. Verma, C. Kang, Y. Pai, T. Chen, J. Yang, C. Sher, Y. Yang, P. Lee, C. Lin, Y. Wu, S. K. Sharma, T. Wu, S. Chung, H. Kuo, Photon. Res. **7**, 579(2019).
[33] M. J. Fan, Y. C. Zhang, X. F. Xie, Y. Chen, D. Pan, S. H. Yan, Optoelectron. Adv. Mat. **16**(7-8), 287 (2022).
[34] L. Sharma, R. Sharma, Optoelectron. Adv. Mat. **16**(7-8), 300 (2022).
[35] P. T. That, P. X. Le, L. V. Tho, H. Y. Lee, Optoelectron. Adv. Mat. **16**(1-2), 68 (2022).

*Corresponding author: nlthai@ntt.edu.vn